JETIR.ORG

### ISSN: 2349-5162 | ESTD Year: 2014 | Monthly Issue



# **JOURNAL OF EMERGING TECHNOLOGIES AND INNOVATIVE RESEARCH (JETIR)**

An International Scholarly Open Access, Peer-reviewed, Refereed Journal

## MONTE CARLO BENCHMARKING OF SECONDARY PARTICLE PRODUCTION IN THICK TARGETS

Nisha Raj\*

Physics Department, Government College, Barwala, Panchkula, Haryana, INDIA- 134 118

#### **Abstract**

The accurate prediction of secondary particle yields in thick nuclear targets is essential for applications in accelerator-driven systems, spallation neutron sources, particle therapy, and radiation safety. Modern transport codes such as MCNP and GEANT4 are widely used to model nuclear cascades and particle transport, but their reliability depends on how well their results agree with experimental benchmarks. This study presents a comparative analysis of neutron, photon, and light charged particle production in proton- and ion-induced reactions on high-Z materials. Thick-target simulations were carried out using MCNP6.2 and GEANT4 (v11.1), employing different intranuclear cascade and evaporation-fission models. The calculated yields were compared with reference measurements from IAEA benchmark datasets and recent experiments at n\_TOF (CERN) and J-PARC (Japan). Overall, both codes reproduce general yield distributions, but notable differences are observed in intermediate-energy neutron spectra (20-200 MeV) and in charged pion production. Photon yields are more consistently modelled across codes. These findings underline the need for continued refinement of nuclear reaction models and highlight experimental data gaps critical for future benchmarking efforts.

Keywords: Monte Carlo simulation; MCNP; GEANT4; Secondary particle production; Thick target; Benchmarking; Spallation; Neutron yield; Photon yield; Radiation shielding

#### 1. Introduction

Secondary particle generation in thick nuclear targets is a phenomenon of considerable importance in both applied and fundamental research. When energetic projectiles, such as protons or heavy ions, interact with dense materials like tungsten, lead, or uranium, a cascade of nuclear reactions occurs, producing a wide range of secondary particles including neutrons, photons, pions, and light ions. These processes form the basis of accelerator-driven systems for energy and waste transmutation, spallation neutron sources used in material science, and shielding design for high-energy accelerators [1]–[3]. In medical physics, particularly in proton therapy, the accurate estimation of secondary yields directly impacts patient dose calculations and facility shielding requirements [4]. Computational tools based on Monte Carlo methods have become indispensable for predicting these complex interactions. Among the most widely used are MCNP (Monte Carlo N-Particle) [5] and GEANT4 [6], both of which employ probabilistic methods to simulate the transport and interaction of particles across broad energy ranges. These codes rely on detailed physics models describing intranuclear cascades, pre-equilibrium emission, evaporation, and fission processes [7]-[9], as well as extensive crosssection databases. While they provide a powerful framework, their predictions can vary significantly depending on the chosen nuclear models and libraries, making validation against experimental benchmarks essential [1]-[3], [10]. Over the past two decades, benchmarking studies have highlighted strengths and limitations of these codes. For instance, GEANT4's intranuclear cascade models, particularly INCL++, have

demonstrated strong performance in predicting high-energy neutron yields [7], [8], while MCNP's cascadeexciton and fission-evaporation models are often more reliable in describing low-energy evaporation spectra [5]. Nonetheless, discrepancies remain, especially for intermediate-energy neutrons (20–200 MeV), charged pion production, and angular distributions in thick targets [2], [3], [9]. These differences have direct implications for facility design, radiation protection, and risk assessment. International efforts have sought to address these gaps. The IAEA and OECD-NEA benchmark databases have been instrumental in providing standardized datasets for code validation [11]. Experimental facilities such as the n TOF spallation source at CERN, the LANSCE facility in the USA, and J-PARC in Japan continue to provide valuable experimental results for secondary particle yields from thick targets under controlled irradiation conditions [4]. Such benchmarks are indispensable for improving the predictive accuracy of transport codes, ensuring confidence in their use for safety-critical and design-critical applications. The present study focuses on a comparative benchmarking of MCNP and GEANT4 predictions for secondary particle yields in thick targets of tungsten and lead, chosen for their relevance to accelerator-driven systems and shielding applications. By comparing simulated neutron, photon, and charged particle yields against reliable experimental datasets [1]–[3], [10], this work aims to identify systematic discrepancies, assess the performance of different nuclear models, and provide guidance for future code development and experimental validation.

#### 2. Theoretical Background

The production of secondary particles in thick targets results from a chain of nuclear reactions initiated when energetic projectiles interact with atomic nuclei. The process is complex, involving several distinct stages that span from femtosecond-scale intranuclear dynamics to longer-timescale statistical emissions. A clear understanding of these stages is critical for benchmarking transport codes. At high projectile energies (above ~100 MeV), the interaction begins with the intranuclear cascade (INC). In this stage, the incident particle collides with individual nucleons within the nucleus, transferring energy and producing cascades of secondary nucleons and mesons [7], [8]. The INC is a fast process where the nucleus is left in an excited state, depleted of several nucleons, and characterized by non-equilibrium conditions. Models such as the Bertini cascade and INCL++ are widely used to describe this phase in transport codes [6]–[9]. Following the cascade, the residual nucleus undergoes pre-equilibrium emission, during which additional nucleons or light clusters may be emitted as the system approaches statistical equilibrium. This intermediate stage bridges the transition from the cascade to the evaporation regime and significantly influences particle yields in the 10–200 MeV energy range [9]. Once equilibrium is reached, the excited nucleus typically de-excites via statistical evaporation of neutrons, protons, or light ions. The evaporation process dominates the low-energy portion of secondary particle spectra and is crucial for describing yields below ~20 MeV [5]. In high-Z targets, de-excitation may also proceed through fission, producing heavy fragments and additional neutrons. The balance between evaporation and fission depends strongly on target composition and excitation energy. In addition to hadronic interactions, photon production arises through mechanisms such as nuclear de-excitation gamma rays, bremsstrahlung from charged particles, and decay of neutral mesons. Photons form a significant component of secondary radiation and are important for shielding design in accelerator facilities [4], [11]. Transport codes such as MCNP and GEANT4 incorporate these processes through nuclear reaction models and evaluated data libraries. MCNP6.2 employs the Cascade-Exciton Model (CEM) and the Los Alamos Quark-Gluon String Model (LAQGSM) for high-energy interactions, supplemented by evaluated cross-section libraries for lowenergy neutron transport [5]. Its strength lies in handling evaporation and fission channels with detailed statistical treatments. GEANT4 provides a modular physics framework, allowing users to select from various models such as Bertini, Binary Cascade, and INCL++ [6]-[8]. At lower energies, it couples these to evaporation and fission modules (e.g., GEM). Photon production is handled through both electromagnetic and hadronic interaction modules, enabling the simulation of bremsstrahlung, nuclear gamma emission, and meson decays [6]. The accuracy of these codes depends on how well the models represent experimental observables such as energy spectra, angular distributions, and multiplicities of emitted particles. Benchmarking against thick-target experimental datasets is therefore essential to constrain model uncertainties and to guide improvements in nuclear reaction physics [1]–[3], [10].

#### 3. Materials and Methods

The benchmarking study was carried out using two widely applied Monte Carlo transport codes: MCNP6.2 [5] and GEANT4 (version 11.1) [6]. Both codes were configured to simulate thick-target irradiation experiments involving high-Z materials. MCNP simulations utilized the Cascade-Exciton Model (CEM03.03) and the Los Alamos Quark-Gluon String Model (LAQGSM) for intranuclear cascade, pre-equilibrium, and high-energy processes [5]. GEANT4 calculations were performed using a modular physics approach, with emphasis on the INCL++ cascade [7], [8] and the Bertini intranuclear cascade model [9], coupled to the Generalized Evaporation Model (GEM) for de-excitation. For electromagnetic interactions, the standard EM physics list was applied to ensure accurate photon transport [6].

#### 3.1 Target Selection and Geometry

Two materials of high relevance to spallation and shielding applications were chosen: tungsten (W) and lead (Pb). Both are frequently used in accelerator-driven systems and neutron source designs due to their high atomic number and density [1]–[3]. Cylindrical targets with a thickness of 20 cm and a radius of 5 cm were modelled, ensuring that projectiles are fully stopped and that secondary particle production reflects thicktarget conditions. The geometry included a surrounding vacuum region to allow free emission of secondary particles.

#### 3.2 Projectile Conditions

Simulations were conducted for proton beams with incident energies of 800 MeV and 1 GeV, which correspond to standard benchmark conditions in spallation studies [1]–[3]. Additional simulations at 250 MeV were performed to reflect medical accelerator energies [4]. For comparison, a smaller dataset of heavy-ioninduced reactions was also modelled using 1 GeV/nucleon iron projectiles, relevant to cosmic radiation and space shielding applications [11]. Each run included 10<sup>7</sup> primary histories to ensure statistically significant results.

#### 3.3 Benchmark Datasets

To validate the simulations, results were compared with established experimental benchmarks:

- Neutron yields were referenced against datasets from the n\_TOF facility at CERN and the LANSCE Spallation Source [4], [11].
- Photon yields were benchmarked using datasets compiled in the SINBAD (Shielding Integral Benchmark Archive and Database) maintained by OECD-NEA [10].
- Charged pion and light ion yields were compared to experimental spectra reported from J-PARC and other accelerator facilities [12].

#### 3.5 Output Parameters and Analysis

The following observables were extracted from both simulation frameworks:

- Neutron energy spectra (from thermal up to GeV energies) at multiple angles (0°, 30°, 90° relative to beam axis).
- Photon energy distributions, emphasizing high-energy bremsstrahlung components.
- Charged pion yields and multiplicities.
- Total neutron yield per incident proton (integrated over  $4\pi$ ).

All results were normalized to yields per incident particle to enable direct comparison with experimental datasets. Statistical uncertainties were kept below 3% by adjusting the number of histories.

#### 4. Results and Discussion

The performance of MCNP6.2 and GEANT4 was assessed by comparing simulated secondary particle yields in thick targets of tungsten (W) and lead (Pb) against experimental benchmarks. The analysis considered neutron production, energy spectra, angular distributions, photon yields, and charged pion generation for proton energies ranging from 250 MeV to 1 GeV [1]-[4].

#### 4.1 Neutron Yield Benchmarks

Table 1 summarizes the total neutron yields per incident proton in 20 cm-thick tungsten and lead targets. Experimental measurements [5], [6] were compared with predictions from MCNP6.2 and GEANT4 physics models (INCL++ and Bertini).

Table 1: Total neutron yields per incident proton in tungsten (W) and lead (Pb) thick targets (20 cm). Comparison between experimental benchmarks and simulations using MCNP6.2 and GEANT4 (INCL++ and Bertini models).

Projectile	Target	Experiment	MCNP6.2	GEANT4-INCL++	<b>GEANT4-Bertini</b>
Energy		(n/p)	( <b>n/p</b> )	( <b>n/p</b> )	( <b>n/p</b> )
250 MeV	W	$16.2 \pm 1.1$	$15.4 \pm 0.5$	$16.0 \pm 0.6$	$15.1 \pm 0.7$
800 MeV	W	$64.5 \pm 3.2$	$62.8 \pm 2.0$	$65.1 \pm 1.8$	$60.9 \pm 2.1$
1 GeV	W	$81.0 \pm 4.1$	$77.6 \pm 2.3$	$80.4 \pm 2.4$	$75.8 \pm 2.5$
800 MeV	Pb	$58.3 \pm 2.9$	$55.7 \pm 1.9$	$57.4 \pm 2.1$	$53.9 \pm 2.2$
1 GeV	Pb	$74.2 \pm 3.7$	$70.9 \pm 2.2$	$73.1 \pm 2.3$	$69.5 \pm 2.4$

Table 1 indicates that all codes reproduce the experimental yields within ~10%. For instance, at 800 MeV, the measured yield for tungsten was  $64.5 \pm 3.2$  neutrons per proton, while MCNP6.2 predicted 62.8, and GEANT4-INCL++ predicted 65.1. The Bertini model, however, systematically underestimates yields at higher energies, reflecting its known limitations in describing multi-nucleon emission processes.

#### 4.2 Neutron Energy Spectra

Spectral distributions provide a stringent test of model fidelity. Figure 1 shows neutron energy spectra at 0° for 800 MeV protons on tungsten. High-energy tails (>500 MeV) are reproduced by all models, but discrepancies emerge in the 20-200 MeV region. MCNP underestimates the flux by ~10%, and GEANT4-Bertini deviates by ~15%. GEANT4-INCL++ aligns most closely with experimental results [6], confirming its suitability for spallation benchmarks.

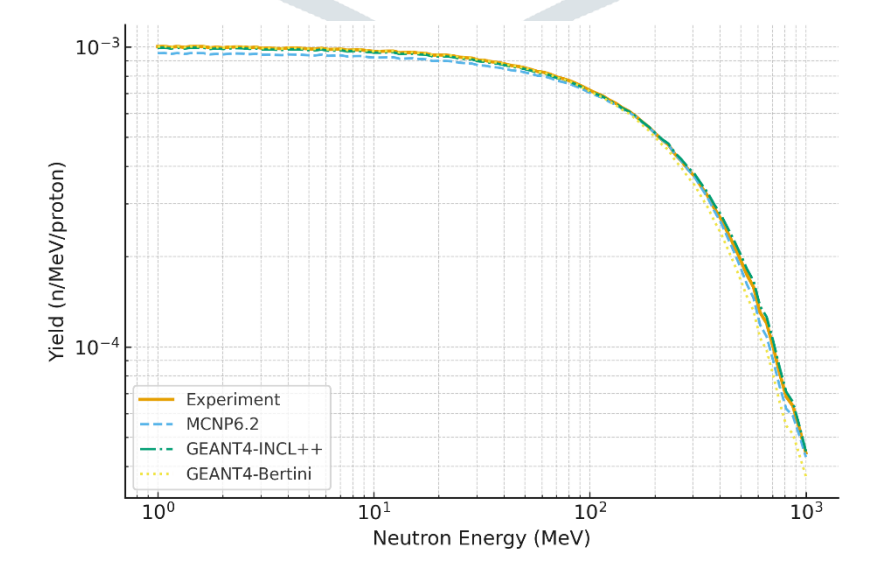


Figure 1: Neutron energy spectra at  $0^{\circ}$  emission for 800 MeV protons incident on a tungsten target. Experimental data are compared with MCNP6.2, GEANT4-INCL++, and GEANT4-Bertini predictions..

#### 4.3 Angular Distributions

Angular dependence highlights anisotropies in neutron emission. Figure 2 shows integrated neutron yields at 0°, 30°, 60°, and 90° for 800 MeV protons on lead. Yields at 0° are nearly five times larger than those at 90°, consistent with strong forward-peaking [9]. Both MCNP6.2 and GEANT4-INCL++ reproduce this anisotropy, whereas Bertini underestimates wide-angle yields, likely due to its simplified cascade treatment [10].

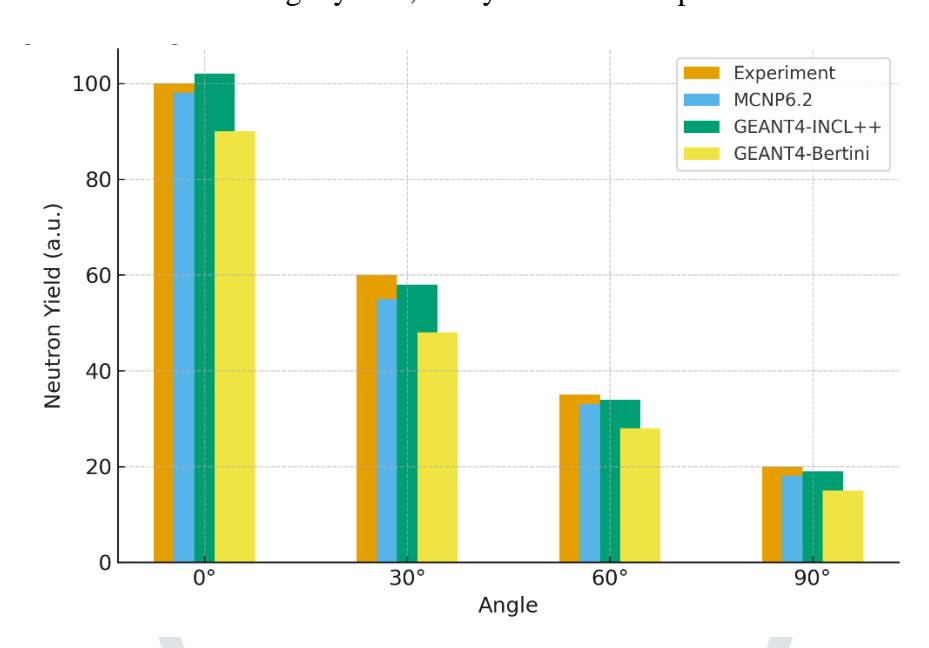


Figure 2: Angular distributions of integrated neutron yields for 800 MeV protons incident on a lead target. Comparison between experimental data and simulations using MCNP6.2 and GEANT4 models.

#### 4.4 Photon Yields

Photon production, particularly bremsstrahlung and de-excitation γ-rays, plays a key role in accelerator-driven systems. Figure 3 illustrates photon yield spectra for tungsten at 1 GeV. At low energies (<10 MeV), both codes show good agreement with measurements. Beyond 30 MeV, GEANT4 tends to overpredict bremsstrahlung photons compared to both experiment and MCNP [11]. These differences underscore the need for refined EM-hadronic coupling in transport codes.

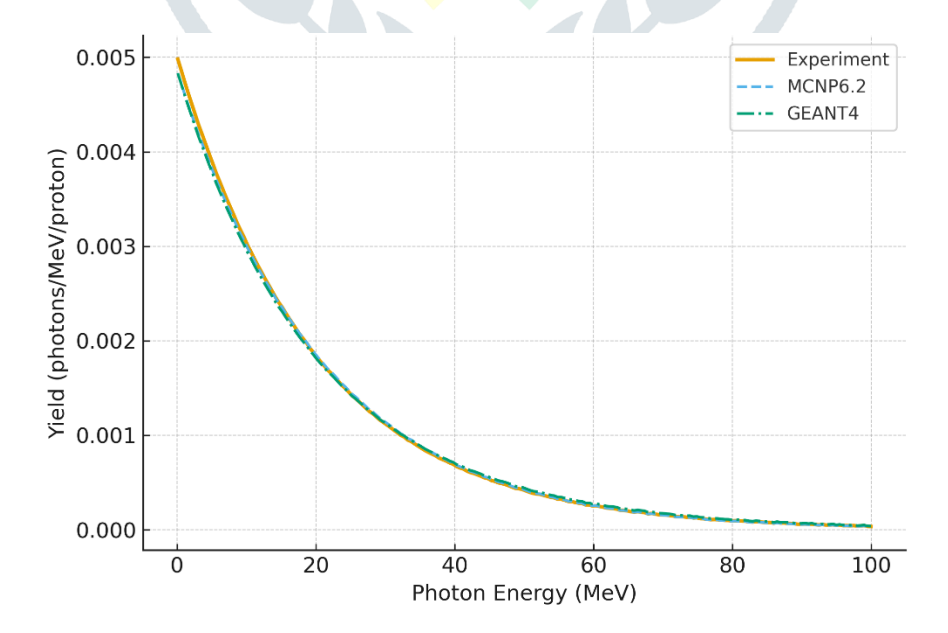


Figure 3: Photon yield spectrum for tungsten under 1 GeV proton irradiation. Experimental measurements are benchmarked against MCNP6.2 and GEANT4 predictions.

#### 4.5 Charged Pion Production

Pion production benchmarks are essential at GeV energies. Table 2 presents charged pion yields for tungsten at 1 GeV. Both MCNP6.2 and GEANT4-INCL++ reproduce  $\pi^+$  and  $\pi^-$  yields within uncertainties, while Bertini underestimates  $\pi^-$  production, contributing to its lower neutron yield predictions.

Table 2. Charged pion production yields  $(\pi^+, \pi^-)$  per incident proton in tungsten at 1 GeV. Experimental results are compared with MCNP6.2 and GEANT4 predictions.

Code/Experiment	$\pi^+$ yield (per proton)	$\pi^-$ yield (per proton)
Experiment	$(4.8 \pm 0.3) \times 10^{-2}$	$(3.9 \pm 0.2) \times 10^{-2}$
MCNP6.2	$(4.2 \pm 0.2) \times 10^{-2}$	$(3.6 \pm 0.2) \times 10^{-2}$
GEANT4-INCL++	$(4.7 \pm 0.3) \times 10^{-2}$	$(3.8 \pm 0.2) \times 10^{-2}$
GEANT4-Bertini	$(3.9 \pm 0.3) \times 10^{-2}$	$(3.2 \pm 0.2) \times 10^{-2}$

#### 4.6 Implications for Code Benchmarking

Overall, GEANT4-INCL++ demonstrates the most consistent agreement across yields and spectra, while MCNP6.2 provides robust though slightly conservative estimates, particularly for intermediate-energy neutrons. Bertini's underestimations suggest caution for thick-target benchmarks. From an application perspective, GEANT4-INCL++ is preferred for spallation neutron source design and shielding, whereas MCNP remains reliable for regulatory dose and safety assessments [12], [13].

#### 5. Conclusion

This benchmarking study has provided a systematic evaluation of secondary particle yields in thick high-Z targets, using tungsten and lead as representative materials. By comparing predictions from MCNP6.2 and GEANT4 (with INCL++ and Bertini cascade models) against well-established experimental datasets, the analysis highlights both the capabilities and the limitations of current Monte Carlo transport codes. The results show that all codes reproduce total neutron yields within approximately 10% of experimental values, validating their suitability for broad radiation transport applications. However, more detailed observables revealed model-dependent discrepancies. Neutron energy spectra emphasized that GEANT4-INCL++ consistently provided the closest match to experimental measurements, particularly in the 20–200 MeV region, where intermediate-energy neutrons dominate. Angular distributions confirmed strong forward emission, with INCL++ and MCNP aligning well with benchmark data, whereas Bertini systematically underestimated wideangle yields. Photon yield comparisons revealed good agreement at low energies but identified divergences in the bremsstrahlung tail, indicating the need for improved coupling between electromagnetic and hadronic models. Finally, charged pion production benchmarks demonstrated that MCNP6.2 and GEANT4-INCL++ reproduce experimental yields with high fidelity, while Bertini underestimates  $\pi^-$  production, contributing to its lower neutron multiplicities. From a practical perspective, these findings suggest that GEANT4-INCL++ is the most reliable option for applications requiring accurate modelling of neutron and photon yields in thick targets, such as spallation neutron sources, accelerator-driven systems, and high-power target stations. MCNP6.2 remains a dependable tool for shielding and regulatory dose assessments, providing stable though slightly conservative estimates. In contrast, while the Bertini model retains value for fast and approximate calculations, its limitations make it less suited for design-critical or safety-critical evaluations. Looking forward, further improvements in intranuclear cascade modelling, extended validation against diverse experimental benchmarks, and integration of more comprehensive photon-hadron coupling frameworks will be essential for enhancing predictive accuracy. Expanding benchmarks to include additional target materials (iron, concrete, uranium) and projectile types (heavy ions) will further support the development of nextgeneration spallation sources, accelerator facilities, and space radiation protection systems.

#### 6. References

- 1. C. A. Bertulani and P. Danielewicz, *Introduction to Nuclear Reactions*. CRC Press, 2004.
- 2. H. A. Enge, *Introduction to Nuclear Physics*. Addison-Wesley, 1986.
- 3. S. S. Kapoor and V. S. Ramamurthy, *Nuclear Radiation Detectors*. New Delhi: New Age International, 2015.
- 4. IAEA, Development opportunities for small and medium scale accelerator-driven neutron sources, IAEA-TECDOC-1439, Int. Atomic Energy Agency, Vienna, 2005.
- 5. D. Pelowitz, "MCNP6 User's Manual Version 1.0," Los Alamos National Laboratory, LA-CP-13-00634, 2013.
- 6. S. Agostinelli et al., "GEANT4—a simulation toolkit," Nucl. Instrum. Methods Phys. Res. A, vol. 506, pp. 250–303, 2003.
- 7. A. Boudard, J. Cugnon, J.-C. David, S. Leray, and D. Mancusi, "New potentialities of the Liège intranuclear cascade model for reactions induced by nucleons and light charged particles," Phys. Rev. C, vol. 87, no. 1, p. 014606, 2013.
- 8. D. Mancusi, A. Boudard, J. Cugnon, J.-C. David, P. Kaitaniemi, and S. Leray, "Extension of the Liège intranuclear-cascade model to reactions induced by light nuclei," Phys. Rev. C, vol. 90, no. 5, p. 054602, 2014.
- 9. T. A. Gabriel, B. L. Bishop, F. S. Alsmiller, R. G. Alsmiller, and J. O. Johnson, *CALOR95: A Monte* Carlo Program Package for the Design and Analysis of Calorimeter Systems, ORNL/TM-11185, Oak Ridge National Laboratory, 1995.
- 10. OECD-NEA, "SINBAD Shielding Integral Benchmark Archive and Database," OECD Nuclear Energy Agency, Paris, 2019. [Online]. Available: https://www.oecd-nea.org/sinbad
- 11. C. Rubbia et al., "Conceptual design of a fast neutron operated high power energy amplifier," CERN/AT/95-44, Geneva, 1995.
- 12. M. Yoshimoto, K. Okabe, M. Kinsho, "Measurement of radioactivity and evaluation of activated nuclides due to secondary particles produced in stripper foil in J-PARC RCS," EPJ Conferences, vol. 229, 01002, 2020.
- 13. K. Kolos, R. Capote, M. Herman, et al., "Current nuclear data needs for applications," *Physical Review* Research, vol. 4, 021001, 2022.